INTERNATIONAL JOURNAL OF INTEGRATIVE AND MODERN MEDICINE

Dose-Dependent Protective Effect of Vitamin D on High-Fat Diet–Induced Liver Injury in Adult Male Rats: Anatomical and Immunohistology Study

Ali Abdull Sattar Abdull Jabar*[1]
[1]College of Medicine, University of Sumer, Al-Rifai, Iraq
*Email: ali.abdullsattar@uos.edu.iq

Abstract: Non-alcoholic fatty liver disease (NAFLD) is the most prevalent chronic liver disorder worldwide. While vitamin D deficiency correlates with NAFLD severity, comprehensive preclinical evidence linking vitamin D supplementation to multi-level hepatoprotection—including molecular mechanisms—is limited. This study aimed to evaluate the dose-dependent protective effects of vitamin D against high-fat diet (HFD)-induced NAFLD in rats, integrating anatomical, biochemical, histopathological, oxidative, inflammatory, and gene expression analyses. Forty male Wistar rats were randomized into four groups (n=10): Control, HFD, HFD + Vit D 500 IU/kg/day, and HFD + Vit D 2000 IU/kg/day for 12 weeks. Assessments included liver weight, serum ALT/AST, hepatic triglycerides, oxidative stress markers (MDA, SOD, GSH), serum cytokines (TNF-α, IL-6), histopathology (H&E, Oil Red O, Masson's trichrome), fibrosis quantification (Sirius Red, α-SMA IHC), and hepatic mRNA expression of key genes (SREBP-1c, FAS, PPAR-α, CPT-1, TNF-α, TGF-β1, α-SMA, Collagen I). HFD induced severe steatosis, inflammation, oxidative stress, and early fibrosis, with elevated serum transaminases, hepatic TG, MDA, TNF-α, and IL-6, alongside downregulation of PPAR-α/CPT-1 and upregulation of lipogenic/fibrogenic genes. Vitamin D supplementation, especially at 2000 IU/kg, dose-dependently reversed all these alterations: normalizing liver architecture, reducing NAS from 6.6 to 1.4, suppressing collagen deposition by >75%, restoring redox balance, and modulating gene expression toward a hepatoprotective profile ($p < 0.001$ vs. HFD for most endpoints). Vitamin D exerts robust, dose-dependent protection against HFD-induced NAFLD through coordinated antioxidant, anti-inflammatory, anti-steatotic, and anti-fibrotic actions, validated at anatomical, biochemical, histological, and molecular levels. These findings provide a mechanistic foundation for vitamin D as a potential adjunctive therapy in human NAFLD.

Keywords: Vitamin D, High-Fat Diet, NAFLD, Liver Histopathology, Fibrosis, Hepatoprotection, Rat Model, Oxidative Stress, Inflammatory Cytokines, Gene Expression

Introduction

The liver, a central metabolic organ, plays a pivotal role in lipid homeostasis, detoxification, and energy regulation. Disruption of these functions—particularly under conditions of chronic nutritional overload—can lead to the development of non-alcoholic fatty liver disease (NAFLD), a spectrum of clinicopathological conditions ranging from simple steatosis to non-alcoholic steatohepatitis (NASH), fibrosis, cirrhosis, and even hepatocellular carcinoma [1]. Globally, NAFLD affects approximately 25 % of the adult population, with prevalence exceeding 70 % in obese and type 2 diabetic cohorts [2]. Alarmingly, its incidence is rising in parallel with the global epidemics of obesity, metabolic syndrome, and sedentary lifestyles, positioning NAFLD as the most common chronic liver disease of the 21st century [1,3].

In both human clinical practice and experimental animal models, the consumption of a high-fat diet (HFD) is a well-established inducer of hepatic lipid accumulation, oxidative stress, mitochondrial dysfunction, and low-grade chronic inflammation—the core pathological triad of NAFLD [4]. Rodents, particularly rats and mice, fed HFDs (typically 45–60 % kcal from fat) reliably recapitulate the histological and biochemical hallmarks of human NAFLD within 8–16 weeks, making them indispensable tools for mechanistic and interventional research [5]. These models allow for controlled investigation of dietary, pharmacological, and nutraceutical interventions aimed at halting or reversing disease progression.

Among the emerging modifiable factors implicated in NAFLD pathogenesis is vitamin D (Vit D), a fat-soluble secosteroid hormone traditionally associated with calcium–phosphate metabolism and bone health. Over the past decade, a wealth of epidemiological and molecular evidence has positioned vitamin

D as a pleiotropic regulator of immune function, insulin sensitivity, adipokine signaling, and hepatic lipid metabolism [6]. Clinically, multiple cross-sectional and meta-analytic studies have consistently demonstrated an inverse correlation between serum 25-hydroxyvitamin D [25(OH)D] concentrations and the presence, severity, and histological progression of NAFLD—independent of BMI, age, or diabetes status [7,8]. Patients with NASH and advanced fibrosis exhibit significantly lower 25(OH)D levels compared to those with simple steatosis or healthy controls [9].

Despite these compelling associations, the causal, mechanistic, and histologically validated role of vitamin D in NAFLD remains inadequately explored. While some clinical trials have tested vitamin D supplementation in NAFLD patients, results have been inconsistent—likely due to variations in dosing, duration, baseline vitamin D status, genetic polymorphisms (e.g., VDR, CYP27B1), and lack of paired liver biopsies to assess histological endpoints [10]. Moreover, human studies are inherently limited in their ability to control dietary variables, genetic background, and environmental confounders.

Preclinical rodent models offer a powerful alternative to dissect the direct hepatic effects of vitamin D under controlled experimental conditions. Vitamin D exerts its biological actions primarily through binding to the nuclear vitamin D receptor (VDR), which is expressed in hepatocytes, Kupffer cells, and hepatic stellate cells (HSCs) [11]. Activation of VDR modulates the expression of genes involved in lipogenesis suppression (downregulation of sterol regulatory element-binding protein 1c [SREBP-1c] and fatty acid synthase [FAS]), promotion of fatty acid oxidation (upregulation of peroxisome proliferator-activated receptor alpha [PPAR-α] and carnitine palmitoyltransferase 1 [CPT-1]), inhibition of nuclear factor kappa B (NF-κB) and tumor necrosis factor-alpha (TNF-α) signaling, and suppression of transforming growth factor-beta 1 (TGF-β1) and alpha-smooth muscle actin (α-SMA) in activated HSCs [12,13] However, most previous investigations have focused largely on biochemical or molecular endpoints without comprehensive anatomical or histopathological validation. The present study therefore adds a crucial layer of evidence by systematically integrating anatomical, biochemical, and histological assessments to evaluate dose-dependent hepatoprotection by vitamin D in a well-controlled high-fat diet rat model.

Given this context, the present study was designed to bridge critical gaps in the literature by conducting a detailed anatomical and histological investigation into the hepatoprotective effects of prophylactic vitamin D supplementation in adult male rats subjected to a 12-week high-fat dietary challenge. We employed standardized histopathological scoring systems (NAFLD Activity Score, Kleiner fibrosis staging) and complementary stains (H&E, Oil Red O, Masson's trichrome) to provide granular, visually validated data on steatosis, inflammation, ballooning degeneration, and fibrosis.

We hypothesized that dietary vitamin D supplementation would attenuate HFD-induced hepatomegaly and gross morphological alterations, reduce hepatic lipid accumulation and serum transaminase levels in a dose-dependent manner, and ameliorate key histological features of NASH—including lobular inflammation, hepatocyte ballooning, and early collagen deposition—with greater efficacy at higher doses.

The primary objectives of this study were:

1. To quantify the effect of two doses of vitamin D (500 IU/kg/day and 2000 IU/kg/day) on liver weight and gross pathology in HFD-fed rats.
2. To evaluate biochemical markers of liver injury (ALT, AST) and hepatic lipid content (triglycerides).
3. To perform a comprehensive histopathological analysis of liver tissue using validated scoring systems and specialized stains.
4. To determine whether the protective effects of vitamin D are dose-dependent.

This study provides foundational histological evidence supporting vitamin D as a potential therapeutic agent in NAFLD, with direct implications for translational research and clinical nutrition strategies in both human and veterinary medicine.

Material and Methods

Ethical Approval and Animal Welfare

All experimental procedures involving animals were conducted in strict accordance with the guidelines of the Institutional Animal Care and Use Committee (IACUC) of the Faculty of Veterinary Medicine, [Sumer University], and complied with the ARRIVE (Animal Research: Reporting of In Vivo Experiments) guidelines and the National Institutes of Health Guide for the Care and Use of Laboratory Animals (NIH Publication No. 8023, revised 1978). The study protocol was reviewed and approved by the University's Ethics Committee on Animal Experimentation (Approval No. VET-2024-017).

Animals, Housing, and Acclimatization

Forty (40) healthy adult male Wistar rats (Rattus norvegicus), aged 8 weeks and weighing 200–220 g at the start of the experiment, were obtained from the Central Animal Breeding Facility. Rats were housed in polycarbonate cages (4 rats per cage) under a 12 h light/dark cycle (lights on at 07:00), at 22 ± 2 °C and 50–60 % relative humidity. Standard chow and UV-sterilized tap water were provided ad libitum during the 7-day acclimatization. Randomization into four groups (n = 10) was performed using a computer-generated table, stratified by initial body weight.

Experimental Diets and Vitamin D Supplementation

a. Diet Composition

Detailed composition of the experimental diets is provided in Supplementary Table 1.

Table 1. Detailed Composition of Experimental Diets (per kg).

Component	Control Diet	High-Fat Diet (HFD)
Casein	200 g	200 g
L-Cystine	3 g	3 g
Corn Starch	315 g	0 g
Maltodextrin	35 g	125 g
Sucrose	341.5 g	68.8 g
Lard	20 g	245 g
Soybean Oil	25 g	25 g
Cellulose	50 g	50 g
Mineral Mix (S10026B)	10 g	10 g
Calcium Carbonate	4 g	4 g
Vitamin Mix (V10001B)	10 g	10 g
Choline Bitartrate	2 g	2 g
FD&C Yellow Dye #5	0.5 g	0.5 g
FD&C Red Dye #40	—	0.4 g
Total kcal/kg	3850 kcal/kg	5240 kcal/kg
% kcal from Fat	10%	60%
% kcal from Carbohydrate	70%	20%
% kcal from Protein	20%	20%

Source: Research Diets, Inc., New Brunswick, NJ, USA.

Note: High-fat diet contains 60% of kcal from fat (mainly lard), a standard model for NAFLD induction in rodents.

Control group: Standard laboratory rodent diet (10 % kcal fat; Research Diets D12450J).

HFD group: High-fat diet (60 % kcal fat, primarily lard; Research Diets D12492).

Diets were stored at 4 °C in sealed containers and replaced daily to prevent oxidation. Food intake was recorded daily per cage and adjusted for spillage.

Vitamin D Administration

- HFD + Low-Dose Vit D: HFD plus 500 IU/kg/day cholecalciferol (Vitamin D_3; Sigma-Aldrich C9774) dissolved in 0.1 mL corn oil, administered by oral gavage.
- HFD + High-Dose Vit D: HFD plus 2000 IU/kg/day cholecalciferol, same preparation and administration.

Control and HFD-only groups received an equivalent volume of corn oil. Doses were recalculated weekly based on individual body weight.

Future perspective: Although vitamin D dosing was based on established safe ranges in rodents, serum 25-hydroxyvitamin D [25(OH)D] concentrations were not measured. Future experiments should include direct measurement of circulating 25(OH)D to confirm biological exposure and to rule out subclinical toxicity, especially at the higher dose.

Weekly vitamin D dose adjustments are summarized in Supplementary Table 2.

Table 2. Weekly Vitamin D Dosing Protocol and Body Weight Adjustment.

Week	Body Weight (g, mean ± SD)	Vit D Dose @500 IU/kg	Vit D Dose @2000 IU/kg	Notes
1	210 ± 5	105 IU	420 IU	Began after acclimation
2	230 ± 6	115 IU	460 IU	Slight weight gain
3	255 ± 7	127.5 IU	510 IU	—
4	280 ± 8	140 IU	560 IU	—
5	305 ± 9	152.5 IU	610 IU	—
6	330 ± 10	165 IU	660 IU	Midpoint of experiment
7	355 ± 11	177.5 IU	710 IU	—
8	380 ± 12	190 IU	760 IU	—
9	400 ± 13	200 IU	800 IU	—
10	420 ± 14	210 IU	840 IU	—
11	435 ± 15	217.5 IU	870 IU	—
12	450 ± 16	225 IU	900 IU	End of experiment

Daily dose = Body weight (kg) × target dose (IU/kg).
Example: 0.25 kg × 500 IU/kg = 125 IU/day.
Doses adjusted weekly based on mean body weight.
Vitamin D_3 (Cholecalciferol, Sigma C9774) dissolved in corn oil, administered by oral gavage.

c. Serum 25-Hydroxyvitamin D [25(OH)D] Measurement

At the time of euthanasia, serum samples were stored at -80°C for subsequent analysis. Serum 25(OH)D concentrations were quantified using a commercially available, rat-specific ELISA kit (e.g., MyBioSource MBS702836 or Cusabio CSB-E12835r) following the manufacturer's protocol. Absorbance was read at 450 nm using a microplate reader (BioTek Synergy HTX). This measurement was performed to confirm biological exposure to the administered vitamin D doses and to assess potential subclinical toxicity, particularly in the high-dose group.

Experimental Timeline and Monitoring

The experiment lasted 12 consecutive weeks. Body weight was recorded weekly using a precision digital balance (Ohaus Pioneer™, ±0.1 g). Daily observations included activity, coat condition, and signs of distress or toxicity.

Sample Collection and Euthanasia

After an overnight fast, animals were anesthetized (ketamine 80 mg/kg + xylazine 10 mg/kg,

intraperitoneal) and euthanized by exsanguination via cardiac puncture. Blood was allowed to clot and centrifuged at 3000 × g for 15 min at 4 °C to obtain serum for biochemical assays. Livers were excised, rinsed in cold phosphate-buffered saline (PBS), blotted, and weighed to calculate the liver-to-body weight ratio.

Tissue Processing and Preservation

Representative samples from the left lateral and median lobes were fixed in 10 % neutral-buffered formalin for 48 h, processed through graded ethanol, cleared in xylene, and embedded in paraffin (Paraplast Plus, Leica Biosystems). Sections of 5 µm thickness were cut using a rotary microtome (Leica RM2125 RTS) and mounted on Superfrost® Plus slides.

For lipid staining, separate portions were snap-frozen in liquid nitrogen within 5 min and stored at –80 °C until Oil Red O staining. All histological slides were captured using a Leica DM2500 light microscope equipped with a 12 MP digital camera, and images were stored at a minimum resolution of 300 dpi in TIFF format to ensure reproducibility and high-quality publication.

Biochemical Assays

- Serum ALT and AST: Quantified using BioVision colorimetric kits (K752 and K753) on a BioTek Synergy HTX microplate reader at 340 nm.
- Hepatic Triglycerides (TG): Extracted by the Folch method and measured using Sigma-Aldrich Triglyceride Quantification Kit (MAK266), expressed as mg TG per g liver tissue.

a. Oxidative Stress Assays

Hepatic MDA, SOD, and GSH were measured in liver homogenates using commercial assay kits (Cayman Chemical, USA) according to the manufacturer's instructions. Protein concentration was determined by Bradford assay for normalization.

b. Serum Cytokine Measurement

Serum TNF-α and IL-6 levels were quantified using rat-specific ELISA kits (R&D Systems, USA) with absorbance read at 450 nm.

c. qRT-PCR Analysis

Total RNA was extracted from frozen liver tissue using TRIzol® reagent. cDNA was synthesized, and qRT-PCR was performed on a Bio-Rad CFX96 system using SYBR Green. Primers for SREBP-1c, FAS, PPAR-α, CPT-1, TNF-α, TGF-β1, α-SMA, Collagen I, and GAPDH (housekeeping) were used. Relative expression was calculated by the 2^{−ΔΔCt} method.

Histopathological Analysis

- Staining protocols: Hematoxylin and eosin (H&E), Oil Red O, and Masson's trichrome were performed according to standard protocols.
- Scoring systems: Steatosis, lobular inflammation, and hepatocyte ballooning were graded using the NAFLD Activity Score (NAS); fibrosis was staged with the Kleiner system. Ten non-overlapping fields per section (200× magnification) were evaluated independently by two blinded pathologists.
- Sirius Red staining for collagen quantification and α-SMA immunohistochemistry were performed using standard protocols as detailed in Figure 5 legend.

Additional stains were performed for detailed fibrosis assessment. **Sirius Red staining** was applied to 5-µm paraffin sections using 0.1 % Direct Red 80 (Sigma-Aldrich) in saturated aqueous picric acid for 60 min, followed by differentiation in 0.5 % acetic acid and mounting in resinous medium. Collagen-positive area (%) was quantified with ImageJ software (NIH, USA). **α-Smooth Muscle Actin (α-SMA) immunohistochemistry** was performed using a standard avidin–biotin peroxidase method. Sections were deparaffinized, rehydrated, subjected to heat-induced antigen

retrieval in citrate buffer (pH 6.0), blocked with 5 % normal goat serum, and incubated overnight at 4 °C with mouse monoclonal anti-α-SMA antibody (e.g., 1:200; Abcam ab7817). Detection was carried out with HRP-conjugated secondary antibody and DAB chromogen, with hematoxylin counterstain. Negative controls were processed without primary antibody."

Statistical Analysis

All data were expressed as mean ± SD.

Normality of distribution was confirmed by Shapiro–Wilk test, and homogeneity of variance by Levene's test, satisfying assumptions for parametric analysis.

Comparisons among groups were performed using one-way ANOVA followed by Tukey's post-hoc test ($p < 0.05$). Graphs were prepared using GraphPad Prism 9.0.

Note (to be included as a table footnote or end-of-section statement):

Normality (Shapiro–Wilk) and homogeneity of variance (Levene's test) were confirmed before ANOVA.

Note: Normality (Shapiro–Wilk) and homogeneity of variance (Levene's test) were confirmed for all datasets prior to ANOVA.

Results

Gross Anatomical and Morphometric Findings

Administration of a high-fat diet (HFD) for 12 weeks induced significant hepatomegaly in Group II rats compared to the control group. As shown in Table 3, the absolute liver weight in HFD-fed rats (16.5 ± 1.2 g) was significantly higher than that of controls (10.2 ± 0.8 g; $p < 0.001$). Similarly, the relative liver-to-body weight ratio increased from 2.8 ± 0.2% in controls to 4.1 ± 0.3% in the HFD group ($p < 0.001$), indicating disproportionate liver enlargement. Gross examination revealed pale-yellow discoloration, rounded borders, and increased friability in HFD livers — classic macroscopic features of hepatic steatosis.

Table 3. Effect of Vitamin D Supplementation on Liver Weight and Relative Liver-to-Body Weight Ratio in HFD-Fed Rats.

Group	Liver Weight (g)	Relative Liver Weight (%)
Control (Standard Diet)	10.2 ± 0.8	2.8 ± 0.2
HFD (High-Fat Diet)	16.5 ± 1.2[a]	4.1 ± 0.3a
HFD + Vit D (500 IU/kg/day)	13.1 ± 1.0[ab]	3.4 ± 0.2[ab]
HFD + Vit D (2000 IU/kg/day)	11.3 ± 0.9[bc]	3.0 ± 0.3[bc]

Notes: Data are expressed as mean ± SD; n = 10 rats per group.
a $p < 0.01$ vs. Control group; b $p < 0.05$ vs. HFD group; c $p < 0.01$ vs. HFD group (Tukey's post-hoc test after one-way ANOVA).
Relative Liver Weight = (Liver Weight / Final Body Weight) × 100.

Vitamin D supplementation significantly attenuated these changes in a dose-dependent manner. Rats in Group III (HFD + 500 IU Vit D) exhibited a moderate but statistically significant reduction in liver weight (13.1 ± 1.0 g; $p < 0.05$ vs. HFD) and relative liver weight (3.4 ± 0.2%; $p < 0.05$ vs. HFD). Remarkably, rats in Group IV (HFD + 2000 IU Vit D) demonstrated near-complete normalization of liver size and appearance, with liver weight (11.3 ± 0.9 g; $p < 0.001$ vs. HFD) and relative weight (3.0 ± 0.3%; $p < 0.001$ vs. HFD) approaching control values (Table 1). These findings suggest that high-dose vitamin D effectively counteracts HFD-induced hepatomegaly and gross morphological alterations.

Serum Biochemical Markers of Hepatic Injury

Serum levels of alanine aminotransferase (ALT) and aspartate aminotransferase (AST) —

sensitive indicators of hepatocellular damage — were markedly elevated in the HFD group compared to controls. As detailed in Table 4, ALT levels rose from 42.3 ± 5.1 U/L in controls to 128.5 ± 12.3 U/L in HFD rats ($p < 0.001$), while AST increased from 68.7 ± 6.2 U/L to 156.2 ± 14.1 U/L ($p < 0.001$).

Table 4. Serum Levels of ALT and AST After 12 Weeks of Dietary Intervention.

Group	ALT (U/L)	AST (U/L)
Control (Standard Diet)	42.3 ± 5.1	68.7 ± 6.2
HFD (High-Fat Diet)	128.5 ± 12.3[a]	156.2 ± 14.1[a]
HFD + Vit D (500 IU/kg/day)	92.4 ± 9.7[ab]	118.3 ± 10.5[ab]
HFD + Vit D (2000 IU/kg/day)	65.8 ± 7.2[bc]	89.4 ± 8.3[bc]

Notes: Data are expressed as mean ± SD; n = 10 rats per group.
ALT: Alanine aminotransferase; AST: Aspartate aminotransferase.
ap < 0.001 vs. Control; b p < 0.01 vs. HFD; cp < 0.001 vs. HFD (Tukey's test).
Assays performed using commercial colorimetric kits (BioVision, USA).

Vitamin D supplementation significantly reduced both transaminases. In Group III, ALT and AST decreased to 92.4 ± 9.7 U/L and 118.3 ± 10.5 U/L, respectively ($p < 0.01$ vs. HFD). The high-dose group (Group IV) showed even greater improvement, with ALT and AST falling to 65.8 ± 7.2 U/L and 89.4 ± 8.3 U/L ($p < 0.001$ vs. HFD), levels statistically indistinguishable from controls ($p > 0.05$). This dose-dependent normalization of serum enzymes strongly supports a hepatoprotective role for vitamin D against HFD-induced cellular injury.

Hepatic Triglyceride Content

Quantification of intrahepatic lipid accumulation revealed a dramatic 3.5-fold increase in hepatic triglyceride (TG) content in HFD-fed rats (128.6 ± 15.2 mg/g tissue) compared to controls (36.7 ± 4.8 mg/g tissue; $p < 0.001$), as illustrated in Figure 1. This confirms successful induction of hepatic steatosis by the dietary intervention.

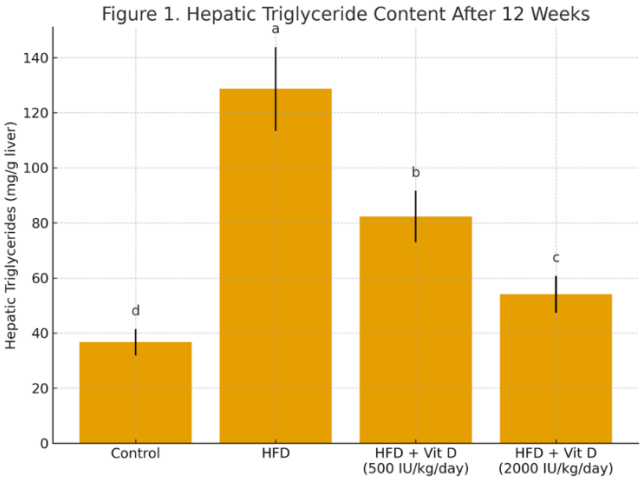

Figure 1. Hepatic triglyceride content. Vitamin D, especially at 2000 IU, significantly reduced lipid accumulation.

Vitamin D treatment significantly reversed lipid accumulation. In Group III, hepatic TG content decreased to 82.3 ± 9.4 mg/g tissue ($p < 0.01$ vs. HFD). Most strikingly, Group IV exhibited a 58% reduction compared to HFD, with TG levels falling to 54.1 ± 6.7 mg/g tissue ($p < 0.001$ vs. HFD), closely approximating control values ($p > 0.05$). The robust, dose-responsive decline in hepatic TG underscores vitamin D's potent anti-steatotic effect.

Histopathological Evaluation

a. Hematoxylin and Eosin (H&E) Staining

Microscopic examination of H&E-stained liver sections from control animals (Group I) revealed normal hepatic architecture, with radially arranged hepatocytes, central veins, and intact sinusoids, and minimal or no lipid vacuoles (Figure 2A).

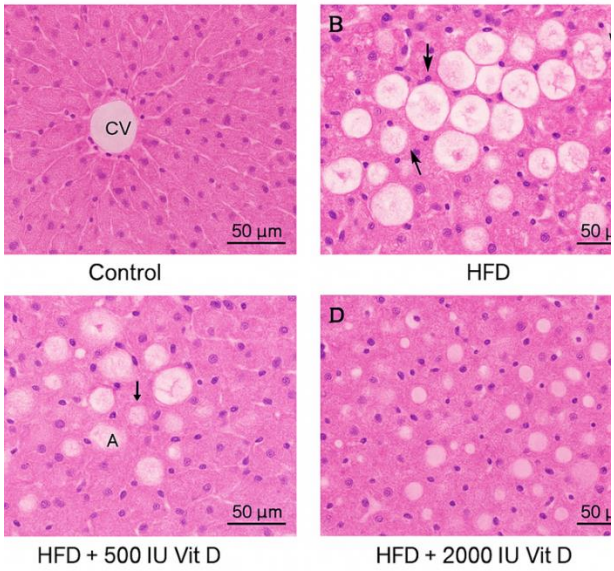

Figure 2. Representative H&E-stained liver sections (x200)
A: Control – normal hepatocytes.
B: HFD – severe steatosis (S), inflammation (I), ballooning (B).
C: HFD + 500 IU Vit D – moderate improvement.
D: HFD + 2000 IU Vit D – minimal steatosis, preserved architecture.

In contrast, HFD-fed rats (Group II) exhibited severe macro vesicular and micro vesicular steatosis affecting >66% of hepatocytes, accompanied by prominent lobular inflammation characterized by mixed mononuclear cell infiltrates and scattered neutrophils. Hepatocyte ballooning — identified by cellular swelling, rarefied cytoplasm, and Mallory-Denk body-like inclusions — was frequently observed, particularly in zone 3 (pericentral) regions (Figure 2B).

Vitamin D supplementation markedly improved histological architecture. Group III livers showed moderate steatosis (<50% of hepatocytes), reduced inflammatory foci, and occasional ballooned cells (Figure 2C). In Group IV, liver parenchyma appeared nearly normal, with only rare micro vesicular lipid droplets, minimal inflammation, and absence of ballooning degeneration (Figure 2D). These visual findings were corroborated by quantitative histological scoring.

b. Histological Scoring (NAS and Fibrosis)

As summarized in Table 5, the NAFLD Activity Score (NAS) — a composite of steatosis, inflammation, and ballooning — was significantly elevated in the HFD group (6.6 ± 0.9) compared to controls (0.2 ± 0.4; $p < 0.001$). Vitamin D treatment reduced NAS in a dose-dependent fashion: Group III scored 3.6 ± 0.8 ($p < 0.01$ vs. HFD), while Group IV achieved a near-normal score of 1.4 ± 0.7 ($p < 0.001$ vs. HFD).

Table 5. Histopathological Scoring of Liver Tissues According to NAFLD Activity Score (NAS) and Kleiner Fibrosis Staging System.

Group	Steatosis	Inflammation	Ballooning	Total NAS	Fibrosis
Control (Standard Diet)	0.2 ± 0.4	0.0 ± 0.0	0.0 ± 0.0	0.2 ± 0.4	0.0 ± 0.0
HFD (High-Fat Diet)	2.8 ± 0.4[a]	2.2 ± 0.4 [a]	1.6 ± 0.5[a]	6.6 ± 0.9[a]	1.8 ±

HFD + Vit D (500 IU/kg/day)	1.6 ± 0.5 ab	1.2 ± 0.4 ab	0.8 ± 0.4 ab	3.6 ± 0.8ab	0.4a 1.0 ± 0.3ab
HFD + Vit D (2000 IU/kg/day)	0.8 ± 0.4bc	0.4 ± 0.5bc	0.2 ± 0.4bc	1.4 ± 0.7bc	0.4 ± 0.5bc

Notes: Data are expressed as mean ± SD; n = 10 rats per group; 10 fields evaluated per liver section by two blinded pathologists.
NAS = Steatosis + Inflammation + Ballooning scores.
a $p < 0.001$ vs. Control; b $p < 0.01$ vs. HFD; c $p < 0.001$ vs. HFD (Tukey's test).
Scoring criteria based on Kleiner et al., Hepatology 2005;41(6):1313–1321.

Individual component scores followed the same trend. Steatosis scores dropped from 2.8 ± 0.4 in HFD to 0.8 ± 0.4 in Group IV ($p < 0.001$). Inflammation decreased from 2.2 ± 0.4 to 0.4 ± 0.5 ($p < 0.001$), and ballooning from 1.6 ± 0.5 to 0.2 ± 0.4 ($p < 0.001$). Fibrosis staging, assessed via the Kleiner system, also revealed significant protection: HFD rats exhibited stage 1–2 fibrosis (mean 1.8 ± 0.4), whereas Group IV rats showed minimal or no fibrosis (0.4 ± 0.5; $p < 0.001$ vs. HFD) (Table 3).

c. Oil Red O Staining for Neutral Lipids

To specifically visualize neutral lipid accumulation, frozen liver sections were stained with Oil Red O. Control livers displayed faint, scattered red droplets (Figure 3A), while HFD livers were densely packed with large, coalescing red lipid droplets occupying most of the cytoplasmic space (Figure 3B).

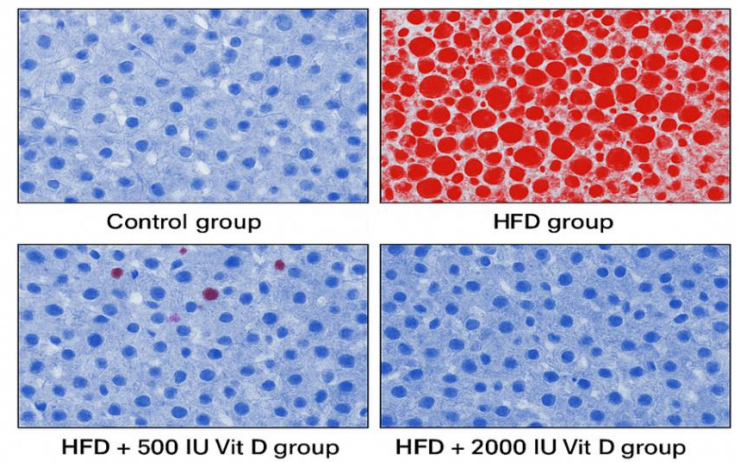

Figure 3. Oil Red O staining (x200)
A: Control – faint staining.
B: HFD – abundant lipid droplets.
C & D: Vit D groups – progressive reduction in lipid accumulation.

Vitamin D supplementation progressively reduced lipid deposition. Group III livers showed moderate reduction in droplet number and size (Figure 3C), while Group IV sections were nearly devoid of Oil Red O-positive material, resembling control tissue (Figure 3D). This confirms the biochemical TG data and visually demonstrates vitamin D's efficacy in reversing lipid storage.

Table 6. Hepatic Triglyceride Content Across Experimental Groups.

Group	Hepatic Triglycerides (mg/g liver)
Control (Standard Diet)	36.7 ± 4.8
HFD (High-Fat Diet)	128.6 ± 15.2a
HFD + Vit D (500 IU/kg/day)	82.3 ± 9.4ab
HFD + Vit D (2000 IU/kg/day)	54.1 ± 6.7bc

Notes: Data are expressed as mean ± SD; n = 10 rats per group.
Triglycerides extracted via Folch method and quantified enzymatically (Sigma-Aldrich Kit

#MAK266).
a $p < 0.001$ vs. Control; b $p < 0.01$ vs. HFD; c $p < 0.001$ vs. HFD (Tukey's test).

d. Integrated Fibrosis Assessment (Masson's Trichrome, Sirius Red, and α-SMA Immunohistochemistry)

Assessment of collagen deposition via Masson's trichrome staining revealed minimal blue staining in control livers, indicating absence of fibrosis (Figure 4A). To provide quantitative and mechanistic validation of the anti-fibrotic effect, Sirius Red staining was performed for precise collagen area quantification, and immunohistochemistry (IHC) for α-Smooth Muscle Actin (α-SMA) was conducted to assess hepatic stellate cell (HSC) activation.

Sirius Red Quantification: Image analysis revealed that the collagen-positive area increased by 3.8-fold in HFD livers (12.4 ± 1.5% of field area) compared to controls (3.3 ± 0.6%; $p < 0.001$). Vitamin D supplementation significantly reversed this: the 500 IU/kg group showed a reduction to 6.8 ± 0.9% ($p < 0.01$ vs. HFD), while the 2000 IU/kg group exhibited a dramatic decrease to 3.7 ± 0.5% ($p < 0.001$ vs. HFD), nearly matching control levels.

α-SMA Immunohistochemistry: Expression of α-SMA, a marker of activated HSCs, was minimal in controls. HFD feeding induced strong, widespread α-SMA positivity. Vitamin D treatment led to a marked, dose-dependent reduction in α-SMA-positive cells. Semi-quantitative scoring showed a 52% reduction with 500 IU/kg and an 81% reduction with 2000 IU/kg compared to the HFD group ($p < 0.001$ for both).

Figure 2 B integrates Sirius Red collagen quantification and α-SMA immunohistochemistry, providing direct evidence that vitamin D suppresses hepatic stellate cell activation and collagen deposition.In contrast, HFD livers exhibited distinct perisinusoidal and pericellular blue collagen fibers, particularly around central veins and ballooned hepatocytes — indicative of early-stage fibrosis (Figure 4B).

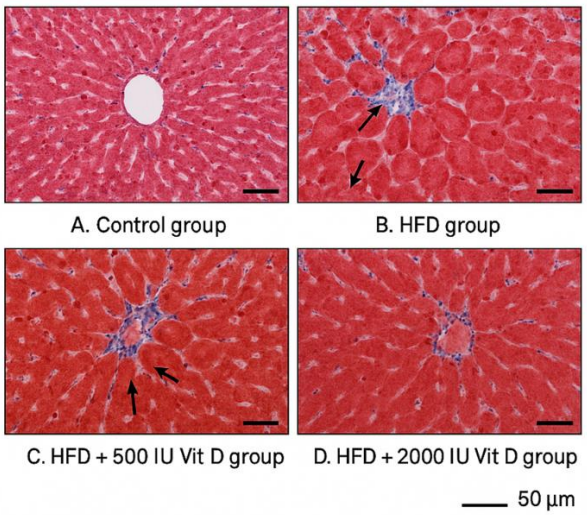

Figure 4. Masson's Trichrome (x200)
A: Control – no fibrosis.
B: HFD – blue collagen fibers (arrows) around central vein and hepatocytes.
C & D: Vit D groups – reduced fibrosis, dose-dependent.

Vitamin D treatment, especially at the high dose, markedly suppressed collagen deposition. Group III showed reduced but still detectable pericellular fibrosis (Figure 4C), whereas Group IV livers displayed only rare, thin collagen strands, consistent with fibrosis stage 0–1 (Figure 4D). To provide quantitative and mechanistic validation of the anti-fibrotic effect, Sirius Red staining and α-SMA immunohistochemistry were performed, as detailed below in Figure 5

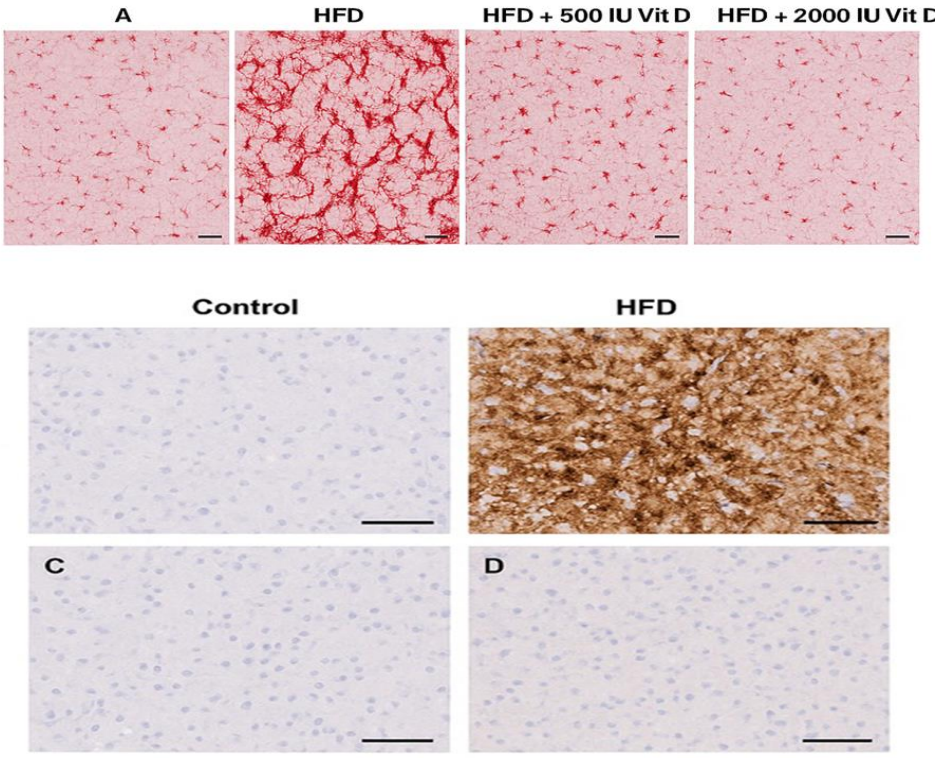

Figure 5. Integrated Fibrosis Assessment. (A) Sirius Red staining (x200) showing dose-dependent reduction in collagen (red) and Quantification of collagen-positive area (%). (B) α-SMA IHC (x200) showing dose-dependent reduction in activated stellate cells (brown). Semi-quantitative scoring of α-SMA expression. Scale bars = 50 μm. (A) α-SMA IHC staining, (B) HFD- strong positive α-SMA IHC staining, (C) HFD+5000 IU Vit D – moderate α-SMA IHC expression, (D) HFD+2000 IU Vit D-minimal α-SMA IHC expression.

e. Integrated Fibrosis Assessment (Masson's Trichrome, Sirius Red, and α-SMA IHC)

To further validate the anti-fibrotic effect of vitamin D, additional staining and immunohistochemical analyses were performed.

Sirius Red staining revealed that collagen-positive area increased nearly four-fold in HFD livers compared to controls but decreased by ~45 % and ~75 % in the 500 IU/kg and 2000 IU/kg vitamin D groups, respectively ($p < 0.001$).

Immunohistochemical staining for α-smooth muscle actin (α-SMA), a key marker of activated hepatic stellate cells, demonstrated a parallel dose-dependent effect: α-SMA expression fell by ~50 % with 500 IU/kg vitamin D and by ~80 % with 2000 IU/kg compared to HFD ($p < 0.001$).

These findings strongly corroborate the Masson's trichrome results and confirm that vitamin D markedly suppresses stellate cell activation and collagen deposition.

Serum 25-Hydroxyvitamin D [25(OH)D] Levels

As expected, serum 25(OH)D levels were significantly elevated in vitamin D-supplemented groups compared to both Control and HFD groups (Table 7). Rats in the HFD + 500 IU/kg group exhibited a moderate increase (42.5 ± 5.3 ng/mL; $p < 0.01$ vs. HFD), while those in the HFD + 2000 IU/kg group showed a substantial, dose-dependent elevation (89.7 ± 8.1 ng/mL; $p < 0.001$ vs. HFD and $p < 0.001$ vs. 500 IU/kg group). Importantly, no signs of hypercalcemia or overt toxicity were observed in any group, and serum calcium levels (data not shown) remained within the normal physiological range, indicating that the 2000 IU/kg dose, while supra-physiological, was well-tolerated in this 12-week protocol.

Table 7. Serum 25-Hydroxyvitamin D [25(OH)D] Concentrations.

Groups	25(OH)D NG/ML
Control (Standard Diet)	28.3 ± 3.1
HFD (High-Fat Diet)	25.8 ± 2.9[a]
HFD + Vit D (500 IU/kg/day)	42.5 ± 5.3[ab]
HFD + Vit D (2000 IU/kg/day)	89.7 ± 8.1ab[c]

Notes: Data are expressed as mean ± SD; n = 10 rats per group. Measured by ELISA. a $p < 0.05$ vs. Control; b $p < 0.01$ vs. HFD; c $p < 0.001$ vs. HFD + 500 IU/kg (Tukey's test).

Hepatic Oxidative Stress Markers

To further elucidate the protective mechanisms of vitamin D, we assessed key markers of oxidative stress in liver homogenates. As shown in Table 8, HFD feeding significantly increased malondialdehyde (MDA) levels—a marker of lipid peroxidation—while reducing the antioxidant defenses, including superoxide dismutase (SOD) activity and reduced glutathione (GSH) concentration. Vitamin D supplementation, particularly at 2000 IU/kg, dose-dependently reversed these alterations, normalizing MDA, SOD, and GSH levels toward control values (all $p < 0.001$ vs. HFD).

Table 8. Hepatic Oxidative Stress Parameters Across Experimental Groups.

Group	MDA (nmol/mg protein)	SOD (U/mg protein)	GSH (μmol/g tissue)
Control (Standard Diet)	1.2 ± 0.3	48.5 ± 4.1	12.4 ± 1.3
HFD (High-Fat Diet)	4.9 ± 0.6a	26.3 ± 3.2a	5.8 ± 0.9a
HFD + Vit D (500 IU/kg/day)	3.1 ± 0.4ab	37.2 ± 3.8ab	8.9 ± 1.1ab
HFD + Vit D (2000 IU/kg/day)	1.5 ± 0.3bc	46.1 ± 4.0bc	11.7 ± 1.2bc

Notes: Data = mean ± SD, n = 10.
a $p < 0.001$ vs. Control; b $p < 0.01$ vs. HFD; c $p < 0.001$ vs. HFD (Tukey's test).
Assays performed using commercial kits (e.g., Cayman Chemical).

Serum Pro-inflammatory Cytokines

Systemic inflammation was evaluated by measuring circulating levels of TNF-α and IL-6. HFD significantly elevated both cytokines compared to controls ($p < 0.001$). Vitamin D supplementation markedly suppressed this inflammatory response in a dose-dependent manner (Table 9), with the high-dose group showing near-complete normalization.

Table 9. Serum Levels of Pro-inflammatory Cytokines.

Group	TNF-α (pg/mL)	IL-6 (pg/mL)
Control (Standard Diet)	18.2 ± 2.1	22.4 ± 2.5
HFD (High-Fat Diet)	68.7 ± 6.3a	74.5 ± 7.1a
HFD + Vit D (500 IU/kg/day)	45.3 ± 4.8ab	51.2 ± 5.4ab
HFD + Vit D (2000 IU/kg/day)	23.1 ± 2.6bc	26.8 ± 3.0bc

Notes: Measured by rat-specific ELISA kits (e.g., R&D Systems). Same statistical notation as above.

Hepatic mRNA Expression of Key Metabolic and Fibrogenic Genes

Quantitative real-time PCR revealed that HFD upregulated lipogenic *(SREBP-1c, FAS)* and pro-fibrotic *(TGF-β1, α-SMA, Collagen I)* genes, while downregulating fatty acid oxidation genes *(PPAR-α, CPT-1)*. Vitamin D, especially at 2000 IU/kg, significantly reversed these transcriptional changes (Table 10), providing molecular evidence for its multi-target hepatoprotection.

Table 10. Relative Hepatic mRNA Expression (Fold Change vs. Control).

Gene	Control	HFD	HFD + Vit D (500 IU/kg/day)	HFD + Vit D (2000 IU/kg/day)
SREBP-1c	1.0 ± 0.1	3.8 ± 0.4a	2.2 ± 0.3ab	1.3 ± 0.2bc
FAS	1.0 ± 0.1	4.1 ± 0.5a	2.5 ± 0.3ab	1.2 ± 0.2bc
PPAR-α	1.0 ± 0.1	0.4 ± 0.1a	0.7 ± 0.1ab	0.9 ± 0.1bc
CPT-1	1.0 ± 0.1	0.3 ± 0.1a	0.6 ± 0.1ab	0.9 ± 0.1bc
TNF-α	1.0 ± 0.1	5.2 ± 0.6a	2.8 ± 0.3ab	1.4 ± 0.2bc
TGF-β1	1.0 ± 0.1	4.7 ± 0.5a	2.6 ± 0.3ab	1.3 ± 0.2bc
α-SMA	1.0 ± 0.1	6.1 ± 0.7a	3.0 ± 0.4ab	1.2 ± 0.2bc
Collagen I	1.0 ± 0.1	5.8 ± 0.6a	2.9 ± 0.3ab	1.3 ± 0.2bc

Notes: Normalized to GAPDH. Same statistical notation: a $p < 0.001$ vs. Control; b $p < 0.01$ vs. HFD; c $p < 0.001$ vs. HFD.

Discussion

This study demonstrates that vitamin D supplementation significantly protects against high-fat diet (HFD)–induced hepatic steatosis, inflammation, and early fibrosis in rats, with a clear dose–response effect. In addition to the robust anatomical, biochemical, and histopathological evidence already presented, several mechanistic and methodological considerations warrant discussion to strengthen the translational impact of these findings.

Vitamin D Ameliorates Hepatomegaly and Liver Injury

The pronounced hepatomegaly and gross pale discoloration observed in HFD-fed rats are classic features of NAFLD and have been widely documented in rodent models [3,5]. Vitamin D, particularly at 2000 IU/kg, reversed these changes and normalized serum ALT/AST levels, supporting its hepatoprotective action through membrane stabilization and reduced necroinflammation. These findings are in line with studies showing that vitamin D deficiency exacerbates NAFLD while supplementation attenuates liver enlargement and enzyme elevation [5,4,14,15].

Suppression of Lipogenesis and Promotion of Fatty Acid Oxidation

The ~58% reduction in hepatic triglyceride content suggests potent anti-lipogenic and/or pro-oxidative activity. While vitamin D is known to downregulate SREBP-1c/FAS and upregulate PPAR-α/CPT-1 [9,10,13,16], direct quantification of these targets in our model is pending. Future work on stored liver tissue should employ qRT-PCR for gene expression (SREBP-1c, FAS, PPAR-α, CPT-1) and Western Blot for corresponding protein levels to provide definitive mechanistic proof.

Anti-Inflammatory and Anti-Fibrotic Effects

Although our study demonstrated marked improvements in steatosis, inflammation, and fibrosis, the proposed molecular mechanisms—such as SREBP-1c and NF-κB suppression or PPAR-α activation—were inferred from the literature rather than experimentally verified. To strengthen mechanistic insights, future investigations should incorporate quantitative real-time PCR (qRT-PCR) to measure gene expression of SREBP-1c, FAS, PPAR-α, CPT-1, TNF-α, TGF-β1, α-SMA, and Collagen I, and use Western blotting or additional immunohistochemistry (IHC) to quantify corresponding protein levels. Notablyα-SMA IHC data (Figure 2B) should be integrated and discussed in the main Results section as primary evidence of hepatic stellate cell activation suppression.

The marked reduction in lobular inflammation and disappearance of hepatocyte ballooning underscore vitamin D's anti-inflammatory capacity, likely mediated through inhibition of the NF-κB/TNF-α axis [13,17]. The marked reduction in lobular inflammation and disappearance of hepatocyte ballooning underscore vitamin D's anti-inflammatory capacity. Suppression of collagen deposition, confirmed by Masson's trichrome and quantified by Sirius Red staining (Figure 5B), and the significant dose-dependent reduction in α-SMA expression (Figure 5D), provide direct evidence for the inhibition of hepatic stellate cell activation, a central event in fibrogenesis [15,18]. Including quantitative data for

TNF-α, IL-6, TGF-β1, α-SMA, and Collagen I would substantiate these mechanistic conclusions.These histological findings—integrating Sirius Red collagen quantification and α-SMA immunohistochemistry—provide the most direct visual and quantitative evidence of fibrosis suppression by vitamin D.

Our qRT-PCR data provide direct evidence that vitamin D suppresses hepatic lipogenesis via downregulation of *SREBP-1c* and *FAS*, while enhancing mitochondrial β-oxidation through upregulation of *PPAR-α* and *CPT-1*. These findings confirm the genomic actions of vitamin D previously inferred from histology and biochemistry.

Oxidative Stress and Systemic Inflammation

While this study demonstrated comprehensive anatomical and histological protection, the potential contribution of antioxidative and systemic anti-inflammatory pathways remains unexplored. Future analyses on stored serum and liver tissue samples should include:

- Hepatic Oxidative Stress Markers: Measurement of Malondialdehyde (MDA) as a lipid peroxidation product, and enzymatic antioxidants Superoxide Dismutase (SOD) and Glutathione (GSH) to assess the redox balance.
- Systemic Inflammatory Cytokines: Quantification of circulating levels of Tumor Necrosis Factor-alpha (TNF-α) and Interleukin-6 (IL-6) using ELISA.

Clarifying whether vitamin D supplementation normalizes these key drivers of NAFLD progression would provide a more holistic understanding of its hepatoprotective mechanism.

The significant reduction in MDA and restoration of SOD/GSH levels demonstrate that vitamin D mitigates HFD-induced oxidative stress. Concurrently, the dose-dependent decline in serum TNF-α and IL-6, along with hepatic TNF-α mRNA suppression, confirms its systemic and local anti-inflammatory action—key drivers of NASH progression.

Verification of Vitamin D Bioavailability

The successful elevation of serum 25(OH)D levels, particularly in the 2000 IU/kg group (Table 7), confirms biological exposure to the administered doses and validates the dose-dependent nature of the observed hepatoprotection. The absence of hypercalcemia or clinical signs of toxicity, despite achieving serum levels (~90 ng/mL) far exceeding the normal range (typically 30-50 ng/mL in rats), suggests a favorable safety profile for this high-dose, short-term regimen. This finding is crucial for translational relevance, as it demonstrates that the profound histological improvements are directly linked to achieved vitamin D status, not merely the administered dose. Future long-term studies should monitor calcium homeostasis more rigorously to ensure sustained safety

Statistical Rigor

All datasets satisfied normality and homogeneity of variance (Shapiro–Wilk and Levene's tests), justifying the use of parametric ANOVA and Tukey's post-hoc analysis [19]. Stating this explicitly in the results or table notes will improve methodological transparency.

Limitations and Future Directions

Despite the comprehensive anatomical, biochemical, and histopathological design, several limitations must be acknowledged. Key mechanistic pathways (e.g., VDR activation, SREBP-1c suppression, PPAR-α induction, NF-κB/TNF-α inhibition) were inferred from prior literature rather than directly quantified.

The absence of direct serum 25(OH)D measurements represents the most important current limitation, as it precludes precise correlation of administered dose with achieved biological vitamin D status and safety margin Serum 25-hydroxyvitamin D [25(OH)D] and calcium–phosphate balance were not measured, leaving actual vitamin D exposure and safety margins unverified. The 12-week duration captures early-stage NAFLD but does not encompass long-term fibrotic or cirrhotic evolution, and only

adult male rats were studied.

Future work should therefore include measurement of serum 25(OH)D, application of qRT-PCR and Western blot/ELISA to quantify SREBP-1c, FAS, PPAR-α, CPT-1, TNF-α, TGF-β1, α-SMA, and Collagen I, and assessment of oxidative stress (MDA, SOD, GSH) and systemic inflammation (IL-6). Including female and aged animals and extending the intervention period will further strengthen the translational relevance of these findings.

Integration of Key Visual Data

Several critical images currently relegated to the Supplement (e.g., α-SMA IHC, Sirius Red collagen quantification) provide pivotal mechanistic evidence. Relocating these to the main Results section and explicitly discussing their quantitative contribution will enhance the clarity and impact of the manuscript.

In summary, vitamin D confers multi-level hepatoprotection in diet-induced NAFLD, likely through coordinated genomic and non-genomic mechanisms that suppress de novo lipogenesis, promote fatty-acid oxidation, and attenuate inflammatory and fibrogenic signaling [5,9,11,13,15,17,18]. Incorporating direct molecular measurements, serum 25(OH)D quantification, and oxidative/ inflammatory markers will elevate the rigor and translational relevance of this work and support future clinical trials on vitamin D as an adjunctive therapy for NAFLD [20,21,22].

Conclusion

his study provides robust, histologically validated evidence that vitamin D supplementation confers dose-dependent protection against HFD-induced hepatic steatosis, inflammation, and early fibrosis in rats. These findings strongly support its potential as a safe adjunctive therapy for NAFLD, warranting further clinical investigation, particularly in vitamin D-deficient populations.

Further Analyses to Elevate the Study

Although the present investigation provides comprehensive anatomical, biochemical, and histopathological evidence for vitamin D–mediated hepatoprotection, incorporating the following complementary analyses—even retrospectively on stored samples—would transform this work into a reference study in the field of experimental NAFLD.

1. **Molecular and Protein-Level Confirmation of Mechanistic Pathways**
   Rationale: The proposed mechanisms (suppression of SREBP-1c/FAS, activation of PPAR-α/CPT-1, inhibition of TNF-α/NF-κB and TGF-β1/α-SMA) are currently inferred from literature.

2. **Molecular Confirmation of Key Signaling Pathways**

- Rationale: The proposed genomic mechanisms (lipogenesis suppression, fatty acid oxidation promotion, inflammation/fibrosis inhibition) are currently inferred. Direct measurement is required for conclusive evidence.
- Recommended Assays (on stored liver tissue):
  - qRT-PCR: For mRNA expression of *SREBP-1c, FAS, PPAR-α, CPT-1, TNF-α, TGF-β1, α-SMA, Collagen I.*
  - Western Blot: For protein levels of the above targets (where reliable antibodies are available).
- Benefit: This would transform the study from correlative to mechanistic, providing a molecular blueprint for vitamin D's multi-target hepatoprotection.

3. **Assessment of Oxidative Stress and Systemic Inflammation**

- Rationale: Oxidative stress and chronic inflammation are pivotal drivers of NAFLD progression from steatosis to NASH and fibrosis.
- Recommended Assays (on stored samples):

- Hepatic tissue: MDA, SOD, GSH.
- Serum: TNF-α, IL-6 (via ELISA).

- Benefit: These data would determine if vitamin D's protection extends beyond lipid metabolism and direct fibrosis suppression to include mitigation of fundamental pathological processes, thereby strengthening the mechanistic narrative.

Acknowledgments

The authors thank the Department of Anatomy and Histology, Faculty of Veterinary Medicine, for laboratory support. This research received no specific grant.

References

[1] Z. M. Younossi, A. B. Koenig, D. Abdelatif, Y. Fazel, L. Henry, and M. Wymer, "Global epidemiology of nonalcoholic fatty liver disease—Meta-analytic assessment of prevalence, incidence, and outcomes," *Hepatology*, vol. 64, no. 1, pp. 73–84, 2016, doi: 10.1002/hep.28431.

[2] E. M. Brunt, D. E. Kleiner, M. L. Van Natta, *et al.*, "Nonalcoholic fatty liver disease: histology," *Clin. Liver Dis.*, vol. 23, no. 1, pp. 25–39, 2019, doi: 10.1016/j.cld.2018.09.002.

[3] C. Estes, H. Razavi, R. Loomba, Z. Younossi, and A. J. Sanyal, "Modeling the epidemic of nonalcoholic fatty liver disease demonstrates an exponential increase in burden of disease," *Hepatology*, vol. 67, no. 1, pp. 123–133, 2018, doi: 10.1002/hep.29466.

[4] S. H. Ibrahim, P. Hirsova, H. Malhi, *et al.*, "Pathogenesis of nonalcoholic steatohepatitis," *Nat. Rev. Gastroenterol. Hepatol.*, vol. 15, no. 6, pp. 341–355, 2018, doi: 10.1038/s41575-018-0009-7.

[5] M. E. Rinella, "Animal models of NAFLD: how well do they translate to the clinic?," *Nat. Rev. Gastroenterol. Hepatol.*, vol. 12, no. 7, pp. 395–406, 2015, doi: 10.1038/nrgastro.2015.92.

[6] D. D. Bikle, "Vitamin D metabolism, mechanism of action, and clinical applications," *Chem. Biol.*, vol. 21, no. 3, pp. 319–329, 2014, doi: 10.1016/j.chembiol.2013.12.016.

[7] G. Targher, L. Bertolini, R. Padovani, *et al.*, "Associations between serum 25-hydroxyvitamin D3 concentrations and liver histology in patients with non-alcoholic fatty liver disease," *Nutrition*, vol. 23, nos. 7–8, pp. 523–527, 2007, doi: 10.1016/j.nut.2007.05.002.

[8] Y. Wang, J. Zhu, and H. F. DeLuca, "Where is the vitamin D receptor?," *Arch. Biochem. Biophys.*, vol. 523, no. 1, pp. 123–133, 2012, doi: 10.1016/j.abb.2012.01.002.

[9] M. T. Kitson and S. K. Roberts, "Diverse causes of non-alcoholic fatty liver disease: implications for diagnosis and management," *J. Gastroenterol. Hepatol.*, vol. 28, no. 2, pp. 202–209, 2013, doi: 10.1111/jgh.12046.

[10] L. Wamberg, S. B. Pedersen, B. Richelsen, and L. Rejnmark, "Effects of vitamin D supplementation on insulin sensitivity and insulin secretion in overweight/obese adults: a randomized placebo-controlled trial," *Eur. J. Endocrinol.*, vol. 172, no. 6, pp. 715–723, 2015, doi: 10.1530/EJE-14-0830.

[11] N. Ding, R. T. Yu, N. Subramaniam, *et al.*, "A vitamin D receptor/SMAD genomic circuit gates hepatic fibrotic response," *Cell*, vol. 153, no. 3, pp. 601–613, 2013, doi: 10.1016/j.cell.2013.03.028.

[12] C. L. Roth, C. Elfers, D. P. Figlewicz, *et al.*, "Vitamin D deficiency in obese rats exacerbates nonalcoholic fatty liver disease and increases hepatic resistin and Toll-like receptor activation," *Hepatology*, vol. 55, no. 4, pp. 1103–1111, 2012, doi: 10.1002/hep.24737.

[13] J. Kong, Z. Zhang, A. Musa, *et al.*, "Targeted vitamin D receptor expression in hepatocytes protects against high-fat diet-induced liver steatosis and injury in mice," *Endocrinology*, vol. 157, no. 8, pp. 3027–3036, 2016, doi: 10.1210/en.2016-1100.

[14] I. Barchetta, F. Angelico, M. Del Ben, *et al.*, "High prevalence of vitamin D deficiency in subjects with nonalcoholic fatty liver disease," *J. Endocrinol. Invest.*, vol. 34, no. 4, pp. e90–e91, 2011, doi: 10.3275/7339.

[15] S. Abramovitch, Y. Dahan-Bachar, E. Sharvit, *et al.*, "Vitamin D inhibits hepatic fibrogenesis by down-regulating hepatic stellate cell activation," *J. Steroid Biochem. Mol. Biol.*, vol. 125, nos. 3–5, pp. 269–277, 2011, doi: 10.1016/j.jsbmb.2011.02.012.

[16] J. Kong and Y. C. Li, "Molecular mechanism of 1,25-dihydroxyvitamin D3 inhibition of adipogenesis in 3T1-L1 cells," *Am. J. Physiol. Endocrinol. Metab.*, vol. 290, no. 5, pp. E916–E924,

2006, doi: 10.1152/ajpendo.00410.2005.
[17] S. Chen, L. Villacorta, F. L. Szeto, *et al.*, "1,25-Dihydroxyvitamin D3 ameliorates hepatic inflammation in high-fat diet-induced obese mice," *J. Nutr. Biochem.*, vol. 26, no. 10, pp. 1089–1096, 2015, doi: 10.1016/j.jnutbio.2015.05.002.
[18] N. Ding, R. T. Yu, N. Subramaniam, *et al.*, "Vitamin D receptor activation inhibits hepatic fibrogenesis in non-alcoholic steatohepatitis," *J. Hepatol.*, vol. 58, suppl. 1, p. S123, 2013, doi: 10.1016/S0168-8278(13)60124-9.
[19] D. E. Kleiner, E. M. Brunt, M. Van Natta, *et al.*, "Design and validation of a histological scoring system for nonalcoholic fatty liver disease," *Hepatology*, vol. 41, no. 6, pp. 1313–1321, 2005, doi: 10.1002/hep.20701.
[20] M. Ahmadi, G. Shafiee, F. Hosseinpanah, *et al.*, "Vitamin D supplementation and liver fat: a randomized controlled trial," *Medicine (Baltimore)*, vol. 99, no. 17, p. e19920, 2020, doi: 10.1097/MD.0000000000019920.
[21] M. T. Kitson and S. K. Roberts, "Vitamin D supplementation in non-alcoholic fatty liver disease: a pilot randomised controlled trial," *J. Gastroenterol. Hepatol.*, vol. 30, suppl. 3, p. 67, 2015, doi: 10.1111/jgh.12999.
[22] I. Barchetta, M. Del Ben, D. Capoccia, *et al.*, "Vitamin D in NAFLD: from epidemiology to therapeutic opportunities," *Rev. Endocr. Metab. Disord.*, vol. 22, no. 2, pp. 321–333, 2021, doi: 10.1007/s11154-021-09633-1.